GENERAL SYMPOSIA | INJECTION MOLDING

Modeling of Polymer Processing of Thermoplastic Polymers: Application to the Injection Molding Process

Vito Speranza, Sara Liparoti, Giuseppe Titomanlio and Roberto Pantani

DOI: https://doi.org/10.51573/Andes.PPS39.GS.IM.5

December 2024

Modeling of Polymer Processing of Thermoplastic Polymers: Application to the Injection Molding Process

Vito Speranza, Sara Liparoti, Giuseppe Titomanlio and Roberto Pantani[1]

Abstract: In the transformation operations of polymeric materials, there is a complex interplay between transport phenomena and crystallization. In particular, the polymer in the molten state is a viscoelastic fluid with rheological parameters depending on temperature, pressure, crystallinity, and molecular stretch. The molecular stretch is a tensor variable with values determined by the history of the flow, temperature, and pressure fields. During polymer processing operations, several phenomena proceed simultaneously by interacting with each other. The combination and interplay of the models that describe each of the phenomena mentioned above provides the evolution of all the relevant quantities and, therefore, also the overall model that describes the evolution of the solidification that generally proceeds starting from the walls (where the temperature is lower and furthermore the shear is higher). This work presents an overall model of the behavior of an isotactic polypropylene during the injection molding process. The model includes the kinetics of spherulitic and fibrillar crystallization and their dependence on the level of molecular stretch; the modeling is carried out up to the prediction of molecular stretch and morphology distributions along the molded part thickness. The model predictions satisfactorily describe the evolution of temperature and pressure during the process and the fundamental aspects of the morphology distribution inside the part.

Keywords: Rapid Heat Cycle Molding (RHCM), Crystallization Kinetics Model, Flow Induced Crystallization, Spherulites' Evolutions, Fibers' Evolutions

1 Vito Speranza (corresponding author)(vsperanza@unisa.it), Sara Liparoti (sliparoti@unisa.it), Giuseppe Titomanlio (gtitomanlio@unisa.it) and Roberto Pantani (rpantani@unisa.it) are affiliated with the Department of Industrial Engineering at the University of Salerno in Italy.

DOI: https://doi.org/10.51573/Andes.PPS39.GS.IM.5

Introduction

Injection molding is a largely adopted transformation process to quickly produce parts with high dimensional accuracy that can be used for a wide range of applications (i.e. automotive, biomedical etc.). Polypropylene (iPP) is one of the most widespread semi-crystalline polymers adopted for such a process. During injection molding, the polymer is melted and is then forced into a (generally) cold cavity in which it solidifies and crystallizes. Finally, it completes its cooling allowing for the part ejection. Performances of the parts can be tailored by properly changing the process conditions. In particular, upon increasing the mold temperature a fast filling of the cavity and a reduction of the molecular stretch can be achieved. However, an increase of the cooling time (and thus of the production time) can occur. To prevent this drawback, the cavity surface temperature can be rapidly heated and cooled during the process. Rapid heat cycle molding (RHCM) processes are designed by adopting several heat sources such as cartridge heaters, steam, or induction coil [1-4]. The part surface defects reduce in the presence of the RHCM and the reproduction accuracy improves with a negligible increase in the cycle time. In semi-crystalline molded parts, the final properties, such as mechanical properties and volumetric shrinkage, are determined by the operating parameters that in turn influence the morphology and crystallinity developed during the process. Several approaches [6,7] were adopted to predict the final properties of the parts by including the crystallization kinetics in the models adopted for injection molding. In particular, a multiscale approach was adopted by Kim and Jeong [7] to predict the spherulite formation. Temperature and flow field were simulated at the macroscale and spherulite growth at the mesoscale. However, these models neglect the material properties evolution induced by the process and the interplay between the material properties.

This work proposes a model for the formation of different morphologies (spherulites and fibers) in an iPP. The model considers the effect of injection molding variables (temperature and pressure) and is coupled with a macromolecular evolution model to consider the effect of flow on crystallinity evolutions through the molecular stretch. The model for the crystallization kinetics has been implemented in the model for the description of the injection molding process previously developed at the University of Salerno (namely UNISA code) [7]. The UNISA code accounts for the interplay between the crystallinity and material properties (i.e. density, viscosity, and relaxation time). The robustness of the model has been proven through comparison with the experimental results in terms of morphology developed along the sample thickness.

Materials and Methods

Injection molding tests were carried out with a commercial grade iPP supplied by Basell, Ferrara, Italy. An extensive characterization campaign was conducted on the iPP. A 1.5 mm thick rectangular cavity was adopted for the tests. To analyze the effect of the cavity surface temperature on the morphology distribution in the part, the conventional injection molding process was coupled

DOI: https://doi.org/10.51573/Andes.PPS39.GS.IM.5

with a rapid heating device. Only a first part of the cavity was covered by the heaters. The RHCM process was implemented by locating thin heaters (240 μm) on both cavity surfaces. A 100 μm steel layer was adopted in order to protect the heaters from the melt contact. A single cavity surface temperature (i.e. 150°C) and two different activation times for the heaters (i.e., 1.3 s and 12 s) were adopted for the injection molding tests.

The numerical simulation of the performed injection molding tests was conducted with the UNISA code, a software developed at the University of Salerno. Such a code considers the filling, packing, and cooling stages. It describes the RHCM process by simultaneously solving the energy balance in both the polymer and the heater. The UNISA code adopts a complete characterization of the iPP. Two competing crystallization kinetics are considered: one for the meso phase and another for the alpha spherulitic phase. The effect of flow on the alpha phase is accounted for. The effect of crystallinity on polymer density, viscosity, and relaxation time is also considered. To predict the different morphologies (fibers and spherulites) of the iPP alpha phase, a recent purpose-built kinetics model [8] was implemented in the UNISA code. The kinetics model describes the competing evolution of fibers and spherulites, for the alpha phase. The effect of flow on nucleation and growth processes of both morphologies is accounted for.

Results

Before checking if simulations correctly describe the final morphology distribution in the part, we will analyze the process evolutions during the process. Figure 1 shows predicted evolutions of process variables for the condition with 150°C cavity surface temperature and 1.3 s heating activation time. It considers the evolutions in a position covered by the heating system, at 15 mm downstream from the cavity entrance.

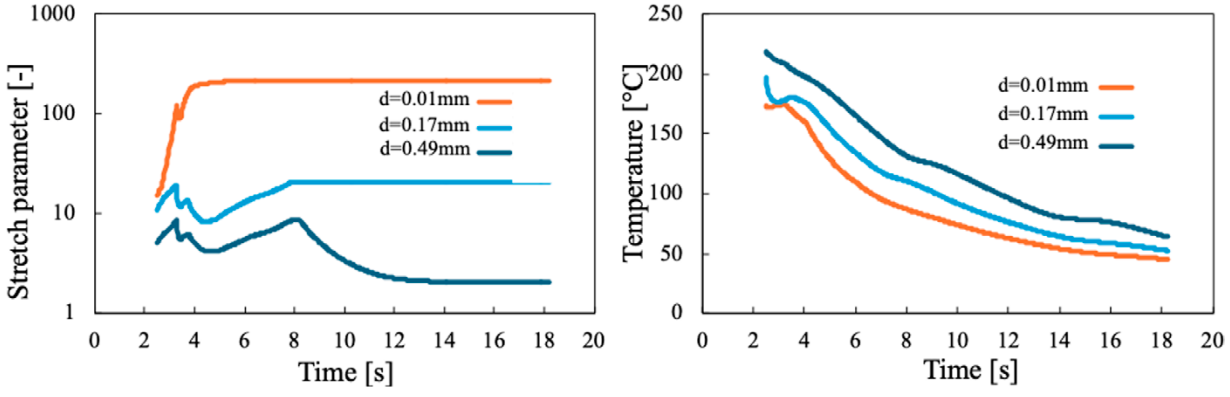

(a) (b)

DOI: https://doi.org/10.51573/Andes.PPS39.GS.IM.5

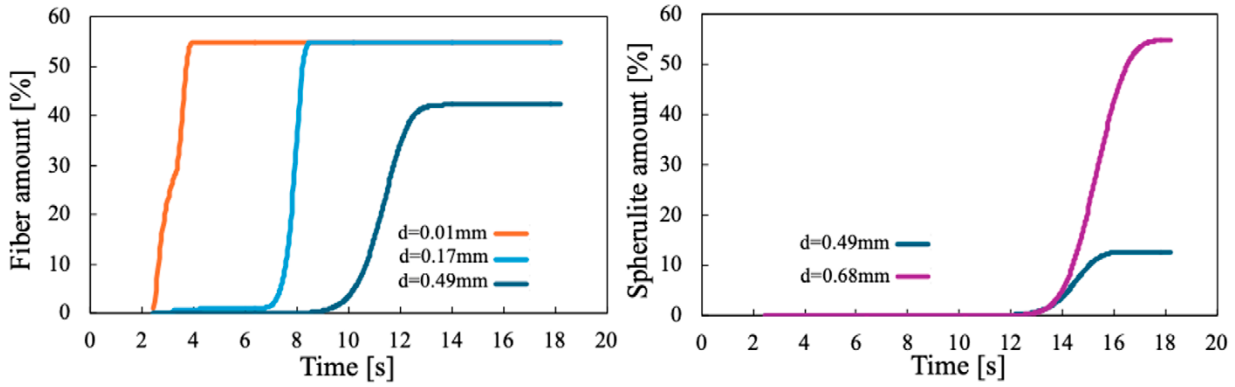

(c) (d)

Figure 1. Predictions at 15 mm downstream from the cavity entrance under the heater system, for the condition with 150°C cavity surface temperature and 1.3 s activation time: (a) stretch parameter, (b) temperature, (c) fiber amount, and (d) spherulite amount.

Figures 1(a-d) report the evolutions of the calculated molecular stretch parameter, temperature, fiber formation, and spherulite formation, respectively, at different distances, d, from the sample surface (0 mm and 0.75 mm identify the sample surface and the sample mid-plane, respectively). The evolutions start from about 2 s, i.e., the time required to the flow front to reach the position. The activation of the heater for the first 1.3 s, after the melt touches the position, limits the cooling to about 150°C for the outer layers of the sample. In Figure 1(a), during the filling, namely up to about 4 s, the stretch increases close to the sample surface (i.e., d=0.01 mm). The fiber formation (see Figure 1[c]) immediately starts and during the filling reaches the maximum allowable degree of crystallinity, namely 55%. The molecular stretch exhibits a plateau when the fibers completely fill the space. Even if the temperature is high, due to the low packing flow and the long relaxation times, induced by the high level of crystallinity, the molecular stretch is essentially constant. In the internal layers (i.e., 0.17 mm and 0.49 mm), the stretch increase during the filling is followed by a stretch decrease during the early stage of packing: the relaxation phenomena, due to the high temperature and the crystallinity absence, efficiently counteracts the effect of flow. During the later stage of packing, although the temperature continues to cool down (see Figure 1[b]), the effect of the packing flow overcomes the relaxation phenomena, determining an increase of the molecular stretch. At d=0.17 mm the fiber formation starts later, at around 6 s, and completes at the end of the packing phase, namely at 8 s. Due to the highest level of crystallinity and the absence of flow, which is characteristic of the cooling phase, the stretch remains constant. Closer to the sample mid-plane, due to the reduced flow and thus low level of stretch, the fiber formation starts during the cooling phase. The simultaneous formation of spherulites (see Figure 1[d]), however, competes with the formation of fibers and both fibers and spherulites fill the available amorphous space. Only spherulites form for distances higher than 0.5 mm.

DOI: https://doi.org/10.51573/Andes.PPS39.GS.IM.5

Figures 2(a-d) show, for the same molding condition, predicted evolutions of variables in the cavity at 100 mm downstream from the cavity entrance, i.e., well outside of the heating system.

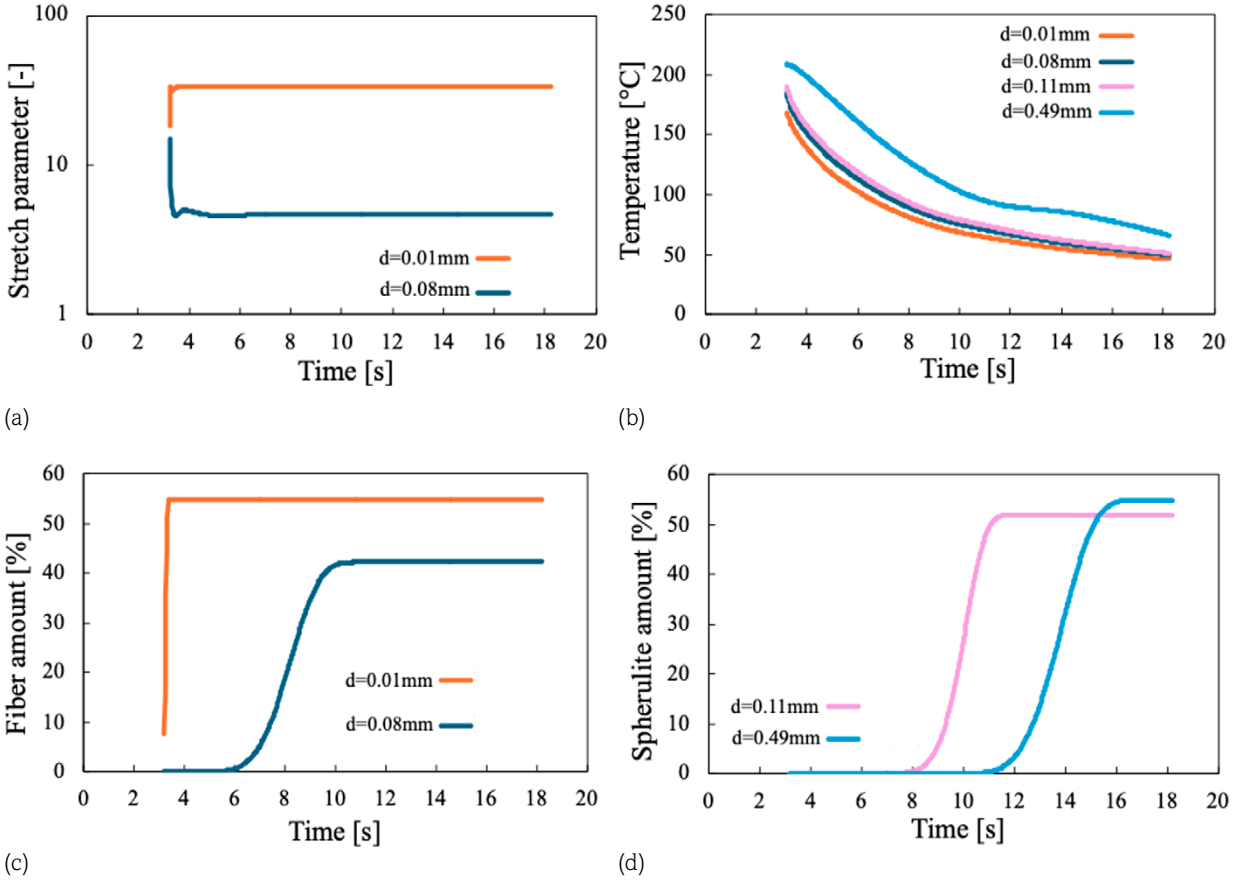

Figure 2. Predictions at 100 mm downstream from the cavity entrance outside of the heating system, for the condition with 150°C cavity surface temperature and 1.3 s activation time: (a) stretch parameter, (b) temperature, (c) fiber amount, and (d) spherulite amount.

The direct contact of the polymer with the unheated mold surface causes a continuous rapid cooling of the material even during the first second of the process (see Figure 2[b]). Due to proximity to the cavity tip, the flow fields are much less intense and the molecular stretch remains remarkably lower (see Figure 2[a]) with respect to the previous position depicted in Figure 1(a). However, very close to the sample surface, a sharp but small increase of the stretch can be observed as soon as the polymer reaches the position; a subsequent stretch plateau corresponding to the fiber evolutions can also be observed. At d=0.08 mm, the level of stretch permits the fiber formation only after 6 s, with a final crystallinity level below 55% (see Figure 2[c]). At inner layers, as the distance from the sample surface increases, only the formation of spherulites occurs with an increasing crystallization time (see Figure 2[d]). Interestingly, the temperature evolution shows an inflection

DOI: https://doi.org/10.51573/Andes.PPS39.GS.IM.5

(see Figure 2[c]), especially at d=0.49 mm, when the material locally crystallizes due to the latent heat generation term accounted for in the energy balance.

Figures 3(a-d) show, at the same position along the flow path considered in Figure 1, i.e., 15 mm downstream from the cavity entrance, the evolutions calculated for the condition with 150°C cavity surface temperature and 12 s heating time.

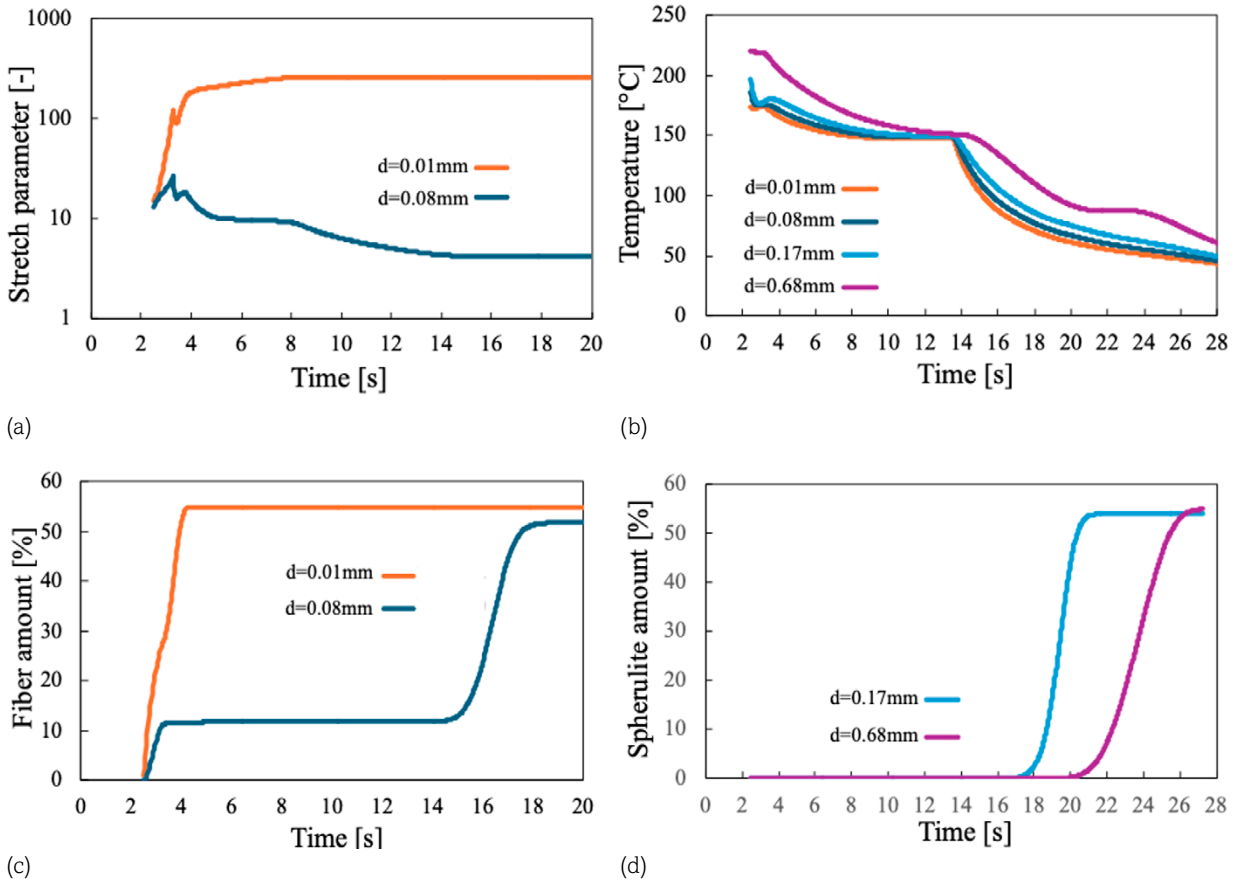

Figure 3. Predictions at 15 mm downstream from the cavity entrance under the heater system, for the condition with 150°C cavity surface temperature and 12 s activation time: (a) stretch parameter, (b) temperature, (c) fiber amount, and (d) spherulite amount.

Close to the sample surface at d=0.01 mm, the stretch evolution (see Figure 3[a]) and fiber formation (see Figure 3[c]) correspond to the ones showed in Figure 1(a) and Figure 1(c), namely calculated for the condition with 1.3 s heating time. The long heating time induces a plateau at about 150°C in the temperature evolutions (see Figure 1[b]). Therefore, after the early stage of packing, at a distance of 0.08 mm from the sample surface, the stretch remains essentially constant (the low packing flow is actively counteracted by the relaxation). The fiber formation starts during filling (see Figure 3[c]),

DOI: https://doi.org/10.51573/Andes.PPS39.GS.IM.5

when the stretch increases, and presents a plateau due to the nearly constant temperature and low stretch; it completes during the second cooling that occurs at the heater deactivation, namely at about 14 s. At d=0.17 mm, spherulite formation occurs during the second cooling (see Figure 3[d]) and all the available space is occupied by spherulitic structures. In the internal layers close to the sample mid-plane, spherulitic crystallization occurs later. An inflection in the temperature evolution is observed when the material locally crystallizes (see Figure 3[b]).

Finally, comparisons between polarized optical micrographs (POM) captured at 15 mm downstream from the cavity entrance and predicted distributions of spherulites and fibers along the sample half thickness are shown in Figure 4.

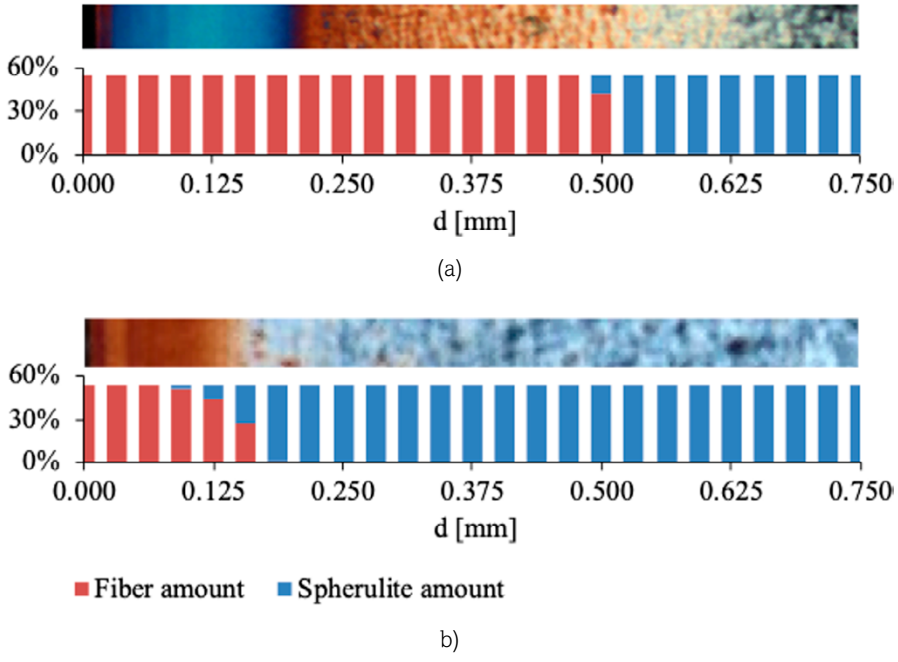

Figure 4. Comparisons between optical micrographs and predicted final morphology distribution along the sample thickness at 15 mm downstream from the cavity entrance, for condition 150°C and 1.3 s (a) for condition 150°C and 12 s (b).

The colored bands in micrographs close to the sample surface are characteristic of the fibrillar layers while the grained area detectable towards the midplane identifies the spherulitic layer. The thickness of such a spherulitic grained area increases as the heating time increases. Coherent with the experimental observations, in the predictions only fibers form close to the sample wall, filling all the local available space; instead, at the sample mid-plane, only spherulites form. The thickness of the fiber and spherulite layers depends on the molding conditions adopted, consistent with experimental observations. In particular, the thickness of the fibrillar layer decreases as the heating time increases. Predicted final morphology distribution correctly describes the experimental

DOI: https://doi.org/10.51573/Andes.PPS39.GS.IM.5

finding in the condition with 12 s heating time while an overestimation of the fibrillar layer thickness is found in the condition with 1.3 s heating time.

Conclusions

An injection molding machine coupled with a rapid heating system was adopted to carry out iPP molding tests under different conditions. The heating system made it possible to control cavity surface temperature and heating system activation time. In particular, two different conditions were considered both with 150°C cavity surface temperature and two heating times: 1.3 s and 12 s. The morphology distributions in the parts were simulated by adopting the UNISA code. The results reasonably predicted the process variable evolutions. The experimental final distribution of morphology, composed by fibers and spherulites, was coherently described by the simulations, especially for long heating activation times. The dependence on molding conditions was also correctly predicted. A slight overestimation of the fibrillar layer thickness was observed for short heating activation times.

References

1. Nian, S.-C., Wu, C.-Y., Huang, M.-S, "Warpage Control of Thin-Walled Injection Molding Using Local Mold Temperatures", *International Communications in Heat and Mass Transfer*, vol. 61, pp. 102–110, 2015, https://doi.org/10.1016/j.icheatmasstransfer.2014.12.008
2. Liparoti, S., Sofia, D., Pantani, R., "Rapid Heating of Mold: Effect of Uneven Filling Temperature on Part Morphology and Molecular Orientation", *Processes*, vol. 11, p. 273, 2023, https://doi.org/10.3390/pr11010273
3. Minh, P.S.; Uyen, T.M.T., Do, T.T., Nguyen, V.-T., Nguyen, V.T.T., "Enhancing the Fatigue Strength of the Weld Line in Advanced Polymer Injection Molding: Gas-Assisted Mold Temperature Control for Thermoplastic Polyurethane (TPU) Composites", *Polymers (Basel)*, vol. 15, p. 2440, 2023, https://doi.org/10.3390/polym15112440
4. Dong, G., Zhao, G., Zhang, L., Hou, J., Li, B., Wang, G., "Morphology Evolution and Elimination Mechanism of Bubble Marks on Surface of Microcellular Injection-Molded Parts with Dynamic Mold Temperature Control", *Industrial & Engineering Chemistry Research*, vol. 57, pp. 1089–1101, 2018, https://doi.org/10.1021/acs.iecr.7b04199
5. Hong, J., Kim, S.K., Cho, Y.-H., "Flow and Solidification of Semi-Crystalline Polymer during Micro-Injection Molding", *International Journal of Heat and Mass Transfer*, vol. 153, pp. 119–576, 2020, https://doi.org/10.1016/j.ijheatmasstransfer.2020.119576
6. Kim, S.K., Jeong, A., "Numerical Simulation of Crystal Growth in Injection Molded Thermoplastics Based on Monte Carlo Method with Shear Rate Tracking". *International Journal of Precision Engineering and Manufacturing*, vol. 20, pp. 641–650, 2019, https://doi.org/10.1007/s12541-019-00089-x

7. Pantani, R., Speranza, V., Titomanlio, G., "Thirty Years of Modeling of Injection Molding. A Brief Review of the Contribution of UNISA Code to the Field", *International Polymer Processing*, vol. 31, pp. 655–663, 2016.

8. Speranza, V., Liparoti, S., Volpe, V., Titomanlio, G., Pantani, R., "Modelling of Morphology Development towards Spherulites and Shish–Kebabs: Application to Isothermal Flow-Induced Crystallization Experiments on Isotactic Polypropylene", *Polymer (Guildf)*, vol. 196, pp. 122–459, 2020, https://doi.org/10.1016/j.polymer.2020.122459